Archives of Virology (2018) 163:1141–1152
https://doi.org/10.1007/s00705-018-3731-z

ORIGINAL ARTICLE

Identification and production of mouse scFv to specific epitope of enterovirus-71 virion protein-2 (VP2)

Jeeraphong Thanongsaksrikul[1] · Potjanee Srimanote[1] · Pongsri Tongtawe[1] · Kittirat Glab-ampai[2] · Aijaz Ahmad Malik[3] · Oratai Supasorn[1] · Phatcharaporn Chiawwit[1] · Yong Poovorawan[4] · Wanpen Chaicumpa[2]

Received: 7 September 2017 / Accepted: 19 December 2017 / Published online: 22 January 2018

Abstract

Enterovirus-71 (EV71) and coxsackievirus-A16 (CA16) frequently cause hand-foot-mouth disease (HFMD) epidemics among infants and young children. CA16 infections are usually mild, while EV71 disease may be fatal due to neurologic complications. As such, the ability to rapidly and specifically recognize EV71 is needed to facilitate proper case management and epidemic control. Accordingly, the aim of this study was to generate antibodies to EV71-virion protein-2 (VP2) by phage display technology for further use in specific detection of EV71. A recombinant peptide sequence of EV71-VP2, carrying a predicted conserved B cell epitope fused to glutathione-S-transferase (GST) (designated GST-EV71-VP2/131-160), was produced. The fusion protein was used as bait in in-solution biopanning to separate protein-bound phages from a murine scFv (MuscFv) phage display library constructed from an immunoglobulin gene repertoire from naïve ICR mice. Three phage-transformed *E. coli* clones (clones 63, 82, and 83) produced MuscFvs that bound to the GST-EV71-VP2/131-160 peptide. The MuscFv of clone 83 (MuscFv83), which produced the highest ELISA signal to the target antigen, was further tested. MuscFv83 also bound to full-length EV71-VP2 and EV71 particles, but did not bind to GST, full-length EV71-VP1, or the antigenically related CA16. MuscFv83 could be a suitable reagent for rapid antigen-based immunoassay, such as immunochromatography (ICT), for the specific detection and/or diagnosis of EV71 infection as well as epidemic surveillance.

Introduction

Enterovirus-71 (EV71) and coxsackievirus-A16 (CA16) often cause hand-foot-mouth disease (HFMD) outbreaks among infants and young children worldwide, including in the Asia–Pacific region where the disease has established endemicity [13]. CA16 infections are mostly asymptomatic or mild and self-limited [11]. In contrast, EV71 frequently causes HFMD with severe neurologic complications that are often fatal [1, 30]. Transmission of causative HFMD viruses occurs by direct contact with blister fluid, saliva, respiratory secretions, and/or the stool of infected subjects [30], and each of these specimen types is suitable for virus detection and case diagnosis. Infected subjects shed the virus in stool and pharyngeal secretions several days before the onset of clinical signs, and also in stool for several weeks during the convalescent period [38]. There are currently no drugs available to treat HFMD. Treatment, therefore, consists of symptomatic and supportive therapy. Licensed vaccines are available only in China [26]. In recent years, EV71 has caused frequent explosive outbreaks with severe symptoms and high fatality [39]. Early and specific diagnostic methods that can

Handling Editor: Tim Skern.

Electronic supplementary material The online version of this article (https://doi.org/10.1007/s00705-018-3731-z) contains supplementary material, which is available to authorized users.

✉ Jeeraphong Thanongsaksrikul
jeeraphong.t@allied.tu.ac.th

[1] Graduate Programme in Biomedical Science, Faculty of Allied Health Sciences, Thammasat University, 99 Moo 18 Paholyothin Road, Klong Luang, Rangsit, Pathum Thani 12120, Thailand

[2] Faculty of Medicine Siriraj Hospital, Center of Research Excellence on Therapeutic Proteins and Antibody Engineering, Mahidol University, Bangkok, Thailand

[3] Faculty of Medical Technology, Center of Data Mining and Biomedical Informatics, Mahidol University, Nakhon Pathom, Thailand

[4] Faculty of Medicine, Center of Excellence in Clinical Virology, Chulalongkorn University, Bangkok, Thailand

differentiate EV71 infection from other enteroviruses, particularly the antigenically-related CA16, are necessary for proper case management and rapid and specific recognition of EV71. Early identification of the presence of EV71 will facilitate the rapid implementation of control measures to limit or even forestall an epidemic.

Enteroviruses are nonenveloped, positive-sense, single-stranded RNA (ssRNA) viruses. The capsid of these viruses comprises the following four structural proteins: surface-exposed VP1, VP2, and VP3, and internal VP4 [36]. VP1 and VP2 are attractive targets for antigen-based immunoassays for disease diagnosis and surveillance [12]. However, VP1 exhibits sequence variability among isolates [24], while VP2 is conserved across EV71 subgenotypes [12]; thus, VP2 is a more suitable diagnostic target. However, antibodies to full-length (FL) EV71-VP2 often cross-react with the CA16 counterpart, as the two viruses share as much as 89% sequence identity at the amino acid level [18, 19]. Given the virulence of EV71, there is an urgent need to identify antibodies that react only with EV71-VP2 for the specific detection of EV71. To that end, a highly conserved linear peptide encompassing a B-cell epitope of EV71-VP2 was predicted, and a recombinant peptide was produced. In this study, mouse single-chain antibody variable-fragments (MuscFvs) that reacted specifically with the FL-EV71-VP2 peptide and EV71 particles, and that did not react to CA16 particles, were produced for further use in an immunoassay for the rapid clinical diagnosis and outbreak surveillance of EV71 infection.

Materials and methods

Viruses

EV71 genotype A (BrCr strain, ATCC®-VR-1775™) and genotype B5 (Thai patient isolate) were propagated in rhabdomyosarcoma (RD) cells (CCL-136™) maintained in complete Dulbecco's Modified Eagle's Medium (DMEM; Biochrom, Cambridge, UK) containing 10% fetal bovine serum, L-glutamine, and antibiotics [37]. The viruses were harvested from the culture supernatants of infected cells that showed ≤ 90% cytopathic effect. Cell culture infectious dose-50 ($CCID_{50}$) of the viruses was determined and calculated using the Kärber formulation [37]. Inactivated CA16 particles were provided by Dr. Alita Kongchanangul of Prof. Dr. Prasert Auewarakul's Laboratory, Institute of Molecular Biosciences, Mahidol University.

Prediction of EV71-VP2 specific B-cell epitope

To predict a specific B-cell epitope within EV71-VP2, the VP2 coding sequences of a EV71 reference strain (GenBank accession number: U22521) as well as Thai isolates (GenBank accession numbers: JF738000, JF738001, and JF738002), a CA16 reference strain (GenBank accession number: U05876.1) and Thai isolates (GenBank accession numbers: JF738003 and JF738004) were retrieved from GenBank (http://www.ncbi.nlm.nih.gov/pubmed/). These were multiply aligned using Clustal Omega multiple sequence alignment program (http://www.ebi.ac.uk/Tools/mas/clustalo/). The EV71-VP2 conserved linear B-cell epitope was predicted from the Immune Epitope Database (IEDB) Analysis Resource (http://tools.iedb.org/main/) using BepiPred Linear Epitope Prediction method [16].

Preparation of recombinant full-length (FL)-EV71-VP1, FL-EV71-VP2, and EV71-VP2 peptide

DNA sequences coding for the FL-EV71-VP1 (297 amino acids; ~ 32 kDa), FL-EV71-VP2 (254 amino acids; ~ 27 kDa), and EV71-VP2 peptide containing the predicted conserved B-cell epitope were amplified from cDNA synthesized from the mRNA of EV71 genotype A. The sequences of the primers used to amplify the genes coding for FL-EV71-VP1, FL-EV71-VP2, and EV71-VP2 peptide are listed in Table 1. FL-EV71-VP1 and FL-EV71-VP2 gene amplicons were directionally cloned into the pQE31 vector (Qiagen, Hilden, Germany). The coding sequence of the EV71-VP2 peptide was cloned in-frame with the glutathione S-transferase (GST) coding sequence, and then deposited into a pGEXT-5T-3 vector (GE Healthcare Life Sciences, Logan, UT, USA). Recombinant plasmids were introduced separately into DH5α *E. coli*. The transformed *E. coli* clones were grown, and the respective DNA inserts of the plasmids were verified by sequencing and Basic Local Alignment Search Tool (BLAST) analysis. Recombinant vectors were used to transform BL21 *E. coli.* Appropriately transformed bacterial clones were grown in IPTG-conditioned Luria–Bertani (LB) broth. N-terminally 6 × His-tagged-FL-EV71-VP1 and FL-EV71-VP2 in bacterial insoluble fractions were solubilized with 100 mM NaH_2PO_4 containing 10 mM Tris–HCl and 8 M urea. Recombinant proteins were purified using Ni–NTA affinity beads (Qiagen) under denaturing conditions. Purified proteins were refolded in PBS and verified by Western blot analysis using mouse monoclonal anti-6 × His (AbD Serotec; Bio-Rad Laboratories, Hercules, CA, USA) to probe the SDS-PAGE-separated proteins. The N-terminally GST-tagged-EV71-VP2 peptide was produced from transformed BL21 *E. coli*, and purified using glutathione resin (Clontech Laboratories, Mountain View, CA, USA). Recombinant GST was produced from *E. coli* carrying empty pGEXT-5T-3 vector and then purified. GST-EV71-VP2 peptide and GST were verified by Western

Table 1 Primer sequences for PCR amplification of the FL-EV71-VP1, FL-EV71-VP2, and EV71-VP2 peptide that contain the specific EV71-VP2 B cell epitope

Primer name	Sequence	Amplicon size (bp)
FL-EV71-VP1	Sense: 5′-GTCGACGGGGACAGAGTGGCAGATG-3′	906
	Anti-sense: 5′-CTGCAGGAGCGTAGTGATTGCCGTTC-3′	
FL-EV71-VP2	Sense: 5′-GTCGACTCTCCCTCTGCTGAAGCATGTG-3′	774
	Anti-sense: 5′-CTGCAGCTGCGTAACTGCCTGCCTGAGAC-3′	
EV71-VP2 peptide	Sense: 5′-GTCGACGTCATTGGAACAGTGGCAGTG-3′	104
	Anti-sense: 5′-GCGGCCGCTTGTAATTCAAATCCATCAGC-3′	

*Sal*I and *Pst*I restriction sites (underlined) were included in the sense and anti-sense sequences of the FL-EV71-VP1 and FL-EV71-VP2 primer sequences, respectively. *Sal*I and *Not*I restriction sites (double underlined) were included in the sense and anti-sense sequences of the EV71-VP2 peptide primer sequence, respectively

blotting (WB) using previously produced rabbit anti-GST to detect both proteins.

Antigenicity of the EV71-VP2 peptide

Commercial mouse anti-EV71 monoclonal antibody (MAB979) (Chemicon; Merck Millipore, Burlington, MA, USA) was used to determine the antigenicity of the GST-EV71-VP2 peptide by means of Western blot analysis. SDS-PAGE-separated antigen was blotted onto nitrocellulose membranes (NCs). The blotted NCs were blocked with 3% bovine serum albumin (BSA), air-dried, and cut vertically into strips. The strips were incubated at 37°C with primary antibody (MAB979; mouse monoclonal anti 6x-His or rabbit anti-GST), washed with pH 7.4 phosphate buffered saline (PBS) containing 0.05% Tween-20 (PBST), and immersed in alkaline phosphatase (AP) conjugated-anti-isotype antibody solution. BCIP/NBT chromogenic substrate (KPL, Inc., Gaithersburg, MD, USA) was used to reveal antigen–antibody reactive bands. The blotted NCs, which were maintained in PBST instead of the primary antibody, served as the negative control.

Construction of the murine scFv (MuscFv) phage display library

Animal experiments received approval from the Institutional Animal Care and Use Committee, Thammasat University, Pathum Thani, Thailand, (COA no. 007/2556). The murine single-chain antibody variable-fragment (MuscFv) phage display library was constructed using three naïve ICR mice (National Laboratory Animal Center, Mahidol University, Salaya, Thailand) and a Mouse IgG Library Primer Set (Progen Biotechnik GmbH, Heidelberg, Germany) [9]. Briefly, the mice were sacrificed by cervical dislocation which was performed by a scientist who holds certificates for the use of laboratory animals in research from the National Research Council of Thailand (NRCT). Spleens were collected, and single splenocytes were prepared. Total RNA was extracted from splenocytes using TRIZol reagent (Thermo Fisher Scientific, Waltham, MA, USA). The quantity and quality of RNA preparations were determined by optical density (OD) ratio (260/280 nm and 260/230 nm, respectively) using a Nanodrop™ spectrophotometer (Thermo Fisher Scientific). High-quality RNA (OD ratios of 260/280 nm and 260/230 nm, and greater than 1.8 and 2, respectively) were treated with deoxyribonuclease (DNase I; Thermo Fisher Scientific) according to the manufacturer's instructions. Complementary DNA (cDNA) was synthesized from mRNA using the Oligo(dT)18 primer and RevertAid Reverse Transcriptase (Thermo Fisher Scientific). Sequence coding for variable domains of immunoglobulin heavy- (*vh*) and light-chains (*vl*) were amplified, cloned in a pSEX81 surface expression phagemid vector (Progen Biotechnik GmbH), and used to transform XL-1 Blue *E. coli* by electroporation according to the manufacturer's instructions. Ten electroporations were performed per one ligation reaction to generate the murine scFv (MuscFv) phage display library. The size of the library was determined from the titers of the transformed *E. coli* colonies grown on a selective agar plate. Bacterial transformants harboring phagemids with MuscFv gene (*muscfv*) inserts were screened by direct colony PCR using sequencing primers that annealed at nucleotide sequences of *pelb* and *gIII* in a pSEX81 phagemid vector. The diversity of amplified *muscfv* sequences was determined by restriction fragment length polymorphism (RFLP) using a *Mva*I restriction enzyme to cut the *muscfvs* (Thermo Fisher Scientific) [32]. Transformed *E. coli* were co-infected with Hyperphages™ (Progen Biotechnik GmbH) to produce complete virions of recombinant phage particles that displayed MuscFv molecules as fusion partners with the phage p3 protein (MuscFv display phages) [2]. The titer of the phage library was determined by counting *E. coli* colony-forming units (CFUs).

Phage biopanning

Selection of phages that displayed EV71-peptide-specific MuscFv was performed by biopanning [32]. GST and GST-EV71-VP2 peptide were immobilized on glutathione resin. The binding capacity of glutathione resin for GST fusion protein is 10 mg/ml resin. For biopanning, 10 µg of GST-EV71-VP2/131-160 (cal. 2.1×10^{14} molecules) was immobilized on 100 µl of glutathione resin. The resin was incubated with rotation with 10^9 CFUs of the MuscFv phage display library. Unbound proteins were washed away with PBS. Empty sites on the resin were blocked with 3% BSA in PBS for 1 h. GST binders in the MuscFv display phage library were removed by incubating the library (10^9 CFUs) with GST-immobilized resin for 1 h. Unbound phages were transferred to incubations with the GST-EV71-VP2 peptide-bound resin. After incubation, resin-unbound phages were discarded and the resin was washed ten times with PBS. All steps were performed at ambient temperature. Phages were eluted from the resin by treatment with trypsin (Sigma-Aldrich, St. Louis, MO, USA) at 37 °C for 15 min. The eluate was incubated with log-phase XL-1 Blue *E. coli* at 37 °C for 15 min to facilitate phage transduction. Transduced bacteria were spread on selective agar plates containing antibiotics. Bacterial transformants harboring *muscfv*-inserted phagemids were screened by direct colony PCR, and the diversity of the *muscfv* sequences was determined by RFLP. MuscFv display phage particles were rescued from each individual *E. coli* culture by co-infecting the bacteria with M13KO7 helper phages (GE Healthcare Life Sciences). The titers of the rescued phages were determined and normalized.

Binding of selected MuscFv display phages to FL-EV71-VP2

MuscFv display phages from bio-panning with the GST-EV71-VP2/131-160 peptide were tested for binding to FL-EV71-VP2 by indirect ELISA using wild-type M13KO7 phages, FL-EV71-VP1, and BSA as control antigens. Individual antigens [1 µg in 100 µl coating buffer (i.e., 0.05 M carbonate-bicarbonate buffer, pH 9.6)] were added to ELISA wells and kept at 37°C until dry. After washing with PBST, all wells were blocked with 200 µl of 3% fetal bovine serum in PBS at 37°C for 1 h. After removing the blocking reagent by washing, normalized MuscFv display phages from individual *E. coli* cultures were added to antigen-coated wells and kept at 25°C for 1 h. The wells were washed with PBST and incubated with mouse anti-M13 monoclonal antibody (GE Healthcare Life Sciences) diluted 1:10,000 in PBST for 1 h, washed, and 100 µl of horse-radish-peroxidase-conjugated anti-mouse isotype (diluted 1:5000 in PBST) was added. After 1 h at 25°C, the secondary antibody was removed by washing before adding ABTS (2,2′-Azinobis [3-ethylbenzothiazoline-6-sulfonic acid]-diammonium salt) chromogenic substrate (KPL, Inc.). The plate was kept at 37°C for 1 h, and then at 4°C overnight. The OD_{405nm} of the content in each well was determined using a microplate reader (Varioskan; Thermo Fisher Scientific) against blank controls (defined as wells to which phage diluents were added instead of MuscFv display phages). MuscFv display phages that yielded $OD405_{nm}$ values with FL-EV71-VP2 greater than 2 × , compared to control antigens, were selected and re-tested for binding to the GST-EV71-VP2 peptide by indirect ELISA. This was similarly performed using GST and M13KO7 phages as control antigens.

Complementarity determining regions (CDRs) and immunoglobulin framework regions (FRs) of *muscfv* sequences from selected MuscFv display phages were determined (IMGT/V-QUEST tool of the International ImMunoGeneTics Information System (IMGT®) [3]. CDRs and immunoglobulin FRs from individual MuscFvs were also aligned using ClustalW2 program.

Production and characterization of soluble MuscFvs

The *muscfv* sequence coding for MuscFv, which gave a high indirect ELISA signal to the GST-EV71-VP2 peptide, was subcloned from the pSEX81-phagemid into the pOPE101-plasmid (Progen Biotechnik GmbH) [31]. XL-1 Blue *E. coli* transformed with *muscfv*-pOPE101 was grown under 20 µM isopropyl β-D-1-thiogalactopyranoside (IPTG) (Amresco/VWR, Radnor, PA, USA) induction conditions at 37 °C and 250 rpm for 5 h. Soluble MuscFv was purified from *E. coli* lysate using Ni–NTA affinity beads, and then checked by SDS-PAGE and WB using mouse monoclonal anti-c-Myc (BioLegend, San Diego, CA, USA).

Antigenic specificity of soluble MuscFv

Purified MuscFv was tested for binding to the GST-EV71-VP2 peptide, FL- EV71-VP2 and GST proteins as well as EV71 and CA16 particles by indirect ELISA. Individual antigens were immobilized in ELISA wells before adding the MuscFv. The ELISA protocol was performed as described in the section "Binding of selected MuscFv display phages to FL-EV71-VP2″. The OD_{405nm} values were determined, and then subtracted from the background binding signal (DMEM-coated well).

For WB, the 12% SDS-PAGE-separated antigens were blotted onto NCs, blocked, and incubated with MuscFv (with c-Myc tag at the C-terminal). Antigen–antibody reactive bands were revealed using AP-conjugated-anti-c-Myc (BioLegend) and BCIP/NBT substrate.

Homology modeling and intermolecular docking

MuscFv sequences were modeled using the I-TASSER server for protein structure and function prediction [10]. The models were subsequently modified [7, 21] to transform them to a condition closer to their native state. The acquired models were validated using PROCHECK Validation of Protein Structure Coordinates [17]. The EV71-VP2 3D structure was modeled based on the crystalline structure (PDB 3VBS). Modeled EV71-VP2 and the MuscFvs were uploaded to the High Ambiguity Driven protein–protein DOCKing (HADDOCK) server to determine their contact interface [14]. The largest docking clusters of the interactive residues with the lowest local energy were selected. Pymol software (PyMOL Molecular Graphics System, Version 1.3r1 edu; Schrodinger, LLC, NY, NY, USA) was used to build models of the interactive proteins.

Results

EV71-VP2 peptide containing a predicted, specific B-cell epitope

Clustal Omega multiple alignments of VP2 sequences of EV71 and CA16 isolates are shown in Fig. 1A. A linear peptide encompassing residues 131-160 (131VIGTVAGGTGTENSHPPYKQTQPGADGFEL160) exhibited characteristics of a B-cell epitope according to the Immune Epitope Database (IEDB) analytical tool and BepiPred Linear Epitope Prediction (Fig. 1B). EV71-VP2 residues I132, V135, T141, K149, Q150, A155, D156, F158, and E159 differed from those of CA16. Specifically, the CA16 residues were L132, I135, N141, V/A 149, T150, Q155, V156, A158, and V159 (Fig. 1A).

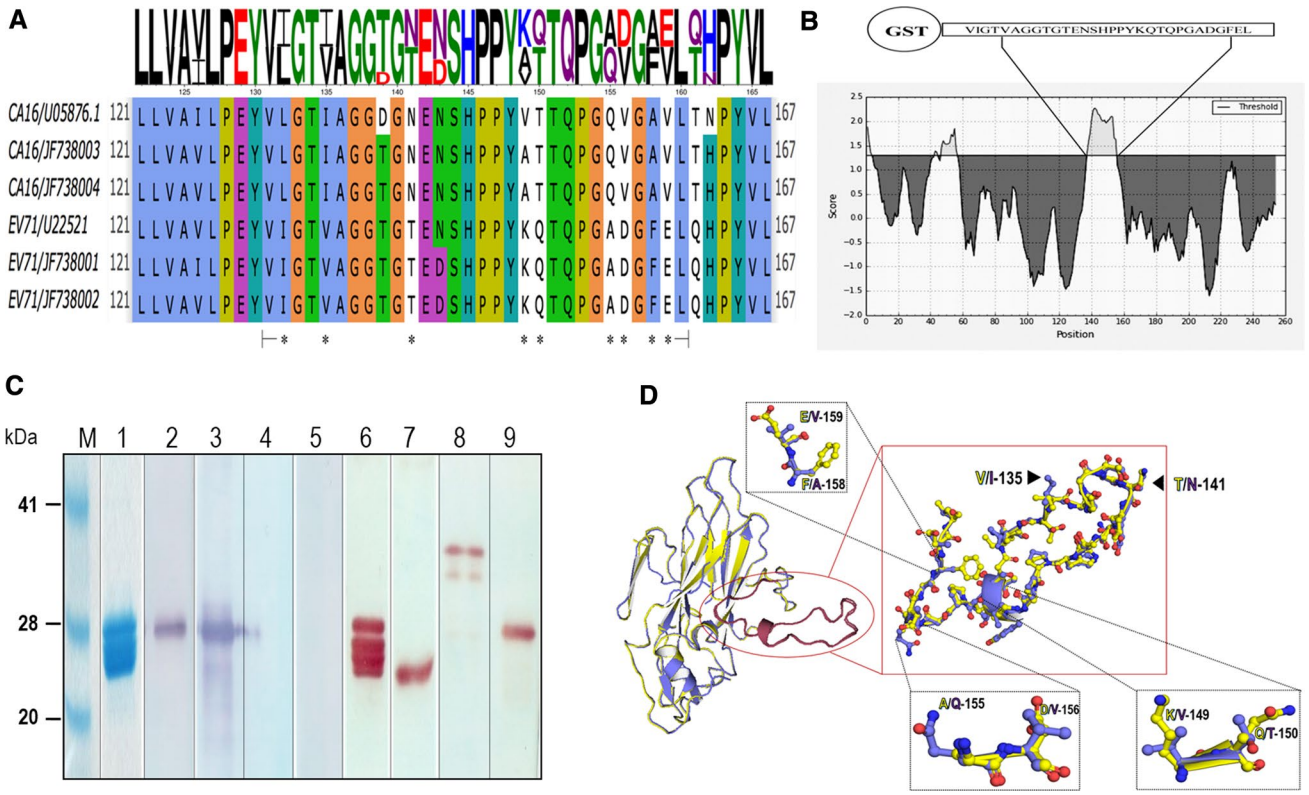

Fig. 1 Prediction and identification of EV71-VP2 B-cell epitopes. **A** Multiple alignments of VP2 sequences from different isolates of EV71 and CA16. Residues 131-160 were predicted to contain an EV71-VP2-specific B-cell epitope. The asterisks indicate EV71-VP2 residues that differ from those of CA16. **B** EV71-VP2/131-160 exhibits linear B-cell epitope characteristics. **C** Antigenicity of GST-EV71-VP2/131-160. CBB-stained SDS-PAGE-separated GST-EV71-VP2/131-160 (lane 1) was bound by commercial EV71-VP2-specific monoclonal antibody (MAB979) (lane 2), which indicated that the protein contains a B-cell epitope. Controls included FL-EV-71-VP2, which was bound by MAB979 (lane 3), and FL-EV71-VP1 and GST, which were not bound by MAB979 (lanes 4 and 5, respectively). GST-EV71-VP2/131-160 and GST were bound by anti-GST (lanes 6 and 7, respectively). Recombinant FL-EV71-VP1 and FL-EV71-VP2 were both bound by an anti-6 × His antibody (lanes 8 and 9, respectively). The multiple reactive bands observed between the SDS-PAGE-separated N-terminally-GST tagged-EV71-VP2/131-160 (lane 1) probed with rabbit polyclonal anti-GST antibody (lane 6) were due to reactions between the polyclonal antibody and the C-terminally truncated (degraded) products of the principal protein. **D** Superimposed picture of the 3D structures of EV71 VP2 (yellow) and CA16 VP2 (magenta)

Thus, the 131VIGTVAGGTGTENSHPPYKQTQPGADGFEL160 sequence (designated EV71-VP2/131-160) is an EV71-VP2-specific sequence.

Recombinant EV71-VP2/131-160

Recombinant EV71-VP2/131-160 fused N-terminally with GST (designated GST-EV71-VP2/131-160) and GST alone were produced, purified, and then analyzed using Western blotting, as shown in Fig. 1C. GST-EV71-VP2/131-160 was bound by MAB979; however, MAB979 did not bind to GST, which indicated that the EV71-VP2/131-160 peptide contained the B-cell epitope. A superimposed image of 3D structures of EV71-VP2 and CA16-VP2 is shown in Fig. 1D. Given that the crystalline structure of the VP2 protein from CA16 has not yet been conclusively identified, the RaptorX structure prediction server (http://raptorx.uchicago.edu/) was used to predict the structure of CA16-VP2.

MuscFv display phage clones that bound to GST-EV71-VP2/131-160

The size of the generated MuscFv phage display library was ~ 1.3×10^8, and 75% of phages in the library contained *muscfv* sequences. After single amplification in the *E. coli* host, ~ 1.41×10^{12} phage particles/ml were obtained. GST-EV71-VP2/131-160-bound phages were selected from the MuscFv phage display library by biopanning, and then used to infect XL-1 Blue *E. coli*. Among the *E. coli* colonies appearing on selective agar plates, 7 *E. coli* clones carried phagemids with non-sibling *muscfv* inserts. Normalized mature phages produced by the 7 *E. coli* clones were first tested for binding to FL-EV71-VP2 using FL-EV71-VP1, with BSA used as a control antigen and MAB979 used as an antibody control. Only phages of *E. coli* clones 63, 82, and 83 significantly bound to FL-EV71-VP2, and did not bind to control antigens (Fig. 2A). Commercialized MAB979 bound with a high ELISA signal to FL-EV71-VP2, and did not bind to FL-EV71-VP1 or BSA. Control anti-6 × His yielded high binding signals to both 6 × His tagged-FL-EV71-VP1 and FL-EV71-VP2. MuscFv63, MuscFv82, and MuscFv83 bound to GST-EV-71-VP2/131-160, and did not bind to GST (Fig. 2B).

MuscFv83 that bound with a relatively high signal to GST-EV71-VP2/131-160 and FL-EV71-VP2 was subcloned from the pSEX81 phagemid into the pOPE101 plasmid, and that plasmid was then transformed into XL-1 Blue *E. coli*. Soluble MuscFv83 was successfully produced and purified from the bacterial lysate (Fig. 3A). MuscFv83 bound to FL-EV71-VP2 and GST-EV71-VP2/131-160, but did not bind to GST by indirect ELISA (Fig. 3B) or Western blotting (Fig. 3C). MuscFv83 also bound to EV71 intact virions, but did not bind to CA16 particles (Fig. 3D).

Computerized interactions between EV71-VP2 and MuscFvs

According to computerized docking models, MuscFv83, which gave a high binding signal to EV71-VP2, used both VH and VL to interact (by different interactive bonds) with specific EV71-VP2 residues within the predicted B-cell epitope sequence. Specific residues included V135, K149, Q150, D156, F158, and E159, which are all specific to EV71-VP2 (Table 2 and Fig. 4). However and importantly, MuscFv63 and MuscFv82 used only the VH domain to bind to 3 and 4 of the EV71-VP2 specific residues, respectively (Table 2 and Supplementary Figs. 1 and 2).

Discussion

Rapid and specific recognition of EV71-infected cases and outbreaks are necessary for prompt clinical management and epidemic control [6, 30, 38]. Conventional methods of EV71 detection include virus isolation followed by serotyping [35], and serotype-specific neutralizing antibody tests to detect seroconversion of paired acute and convalescing sera [8]. However, these methods are time-consuming and labor-intensive. The neutralization test requires stocks of different generated enteroviruses [6]. Moreover, paired sera are often unavailable for the titration of rising antibody responses [28]. Molecular detection methods have been developed, including nested/semi-nested reverse transcription (RT)-PCR that commonly targets the viral 5′ UTR [4, 27, 28, 33, 34]; combined multiplex RT-PCR and diagnostic microarray [5]; and, RT-PCR using consensus degenerate hybrid oligonucleotide primer (CODEHOP) to amplify the VP1 gene, followed by direct DNA sequencing [6, 23]. These methods are more sensitive than virus isolation and serotyping, but they may yield a false-positive result [6]. In addition, these molecular methods require laboratory equipment, expertise, and expensive reagents, which limits their use in low-resource settings. A simple and inexpensive antigen-based test, such as a ready-to-use immunochromatographic kit, would be a more convenient, rapid, affordable, and easy-to-use point-of-care option, all provided that the antibody used as the antigen detector in the system is EV71-specific. Several mouse monoclonal antibodies (MAbs) to EV71 were previously developed. However, they all demonstrated cross-reactivity with CA16 [19, 20], which precluding their use for differential detection of the two viruses. In this study, a different approach to generating EV71-specific

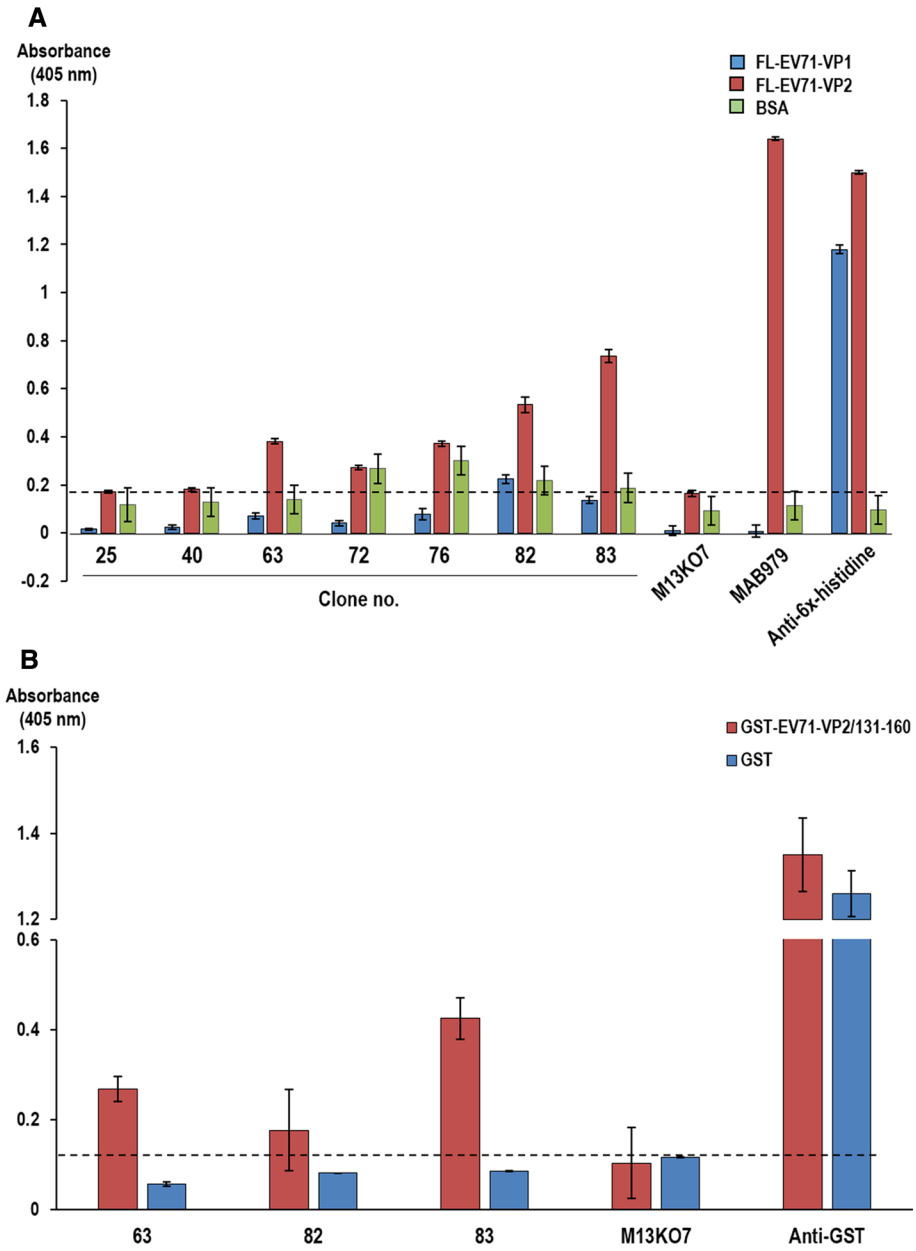

Fig. 2 Screening of MuscFv display phages that bound to the FL-EV71-VP2 and GST-EV71-VP2/131-160 peptide. **A** Indirect ELISA revealed that MuscFv-phages from phage-transformed *E. coli* clones 63, 82, and 83 bound to FL-EV71-VP2 more specifically than they bound to the control antigens (FL-EV71-VP1 and BSA), while the other phage clones were negative, in terms of binding. M13KO phages did not bind to FL-EV71-VP1, FL-EV71-VP2, or BSA. MAB979 bound only to FL-EV71-VP2, and did not bind to FL-EV71-VP1 or BSA. Anti-6x-His antibody bound to both recombinant FL-EV71-VP1 and FL-EV71-VP2. **B** Binding of MuscFvs-phage clones 63, 82, and 83 to GST-EV71-VP2/131-160, but not to GST (by indirect ELISA). M13KO7 and anti-GST were background and positive binding controls, respectively. Each value represents the mean ± standard deviation of ELISA tests performed in triplicate

MAb was employed. EV71-VP2 was selected as the diagnostic target, as this protein is abundant, highly-conserved, and contains an antigenic peptide that differs from the closely related CA16 [12, 19]. From multiple alignments of VP2 sequences of EV71 reference and epidemic strains [25] as well as CA16, we identified a peptide that we designated EV71-VP2/131-160 that contains a predicted B cell epitope, and that has several residues that differ from those of CA16. This peptide was bound by commercial MAB979 to EV71 [19], indicating that it does contain a B-cell epitope.

Phage display technology [29] has paved the way for rapid in vitro production of antibodies specific to any epitopes, regardless of immunogenicity, toxicity, or molecular complexity, in contrast to in vivo immunization processes. Phage clones that display target-bound antibodies can be selected from a library by in vitro biopanning. In this study, a MuscFv display phage library was constructed using ICR mice. Out-bred mice were used to increase the diversity of the antibody repertoire. The library size was ~ 1.3×10^8, with antibody sequence diversity comparable to that of other non-immune libraries [15, 22, 32, 40]. A library is a valuable tool for selecting not only the EV71-VP2-bound-MuscFv display phages, but also for producing MuscFvs to any other epitopes or antigens.

In-solution biopanning of the GST-subtracted MuscFv phage library with GST-EV71-VP2/131-160 immobilized

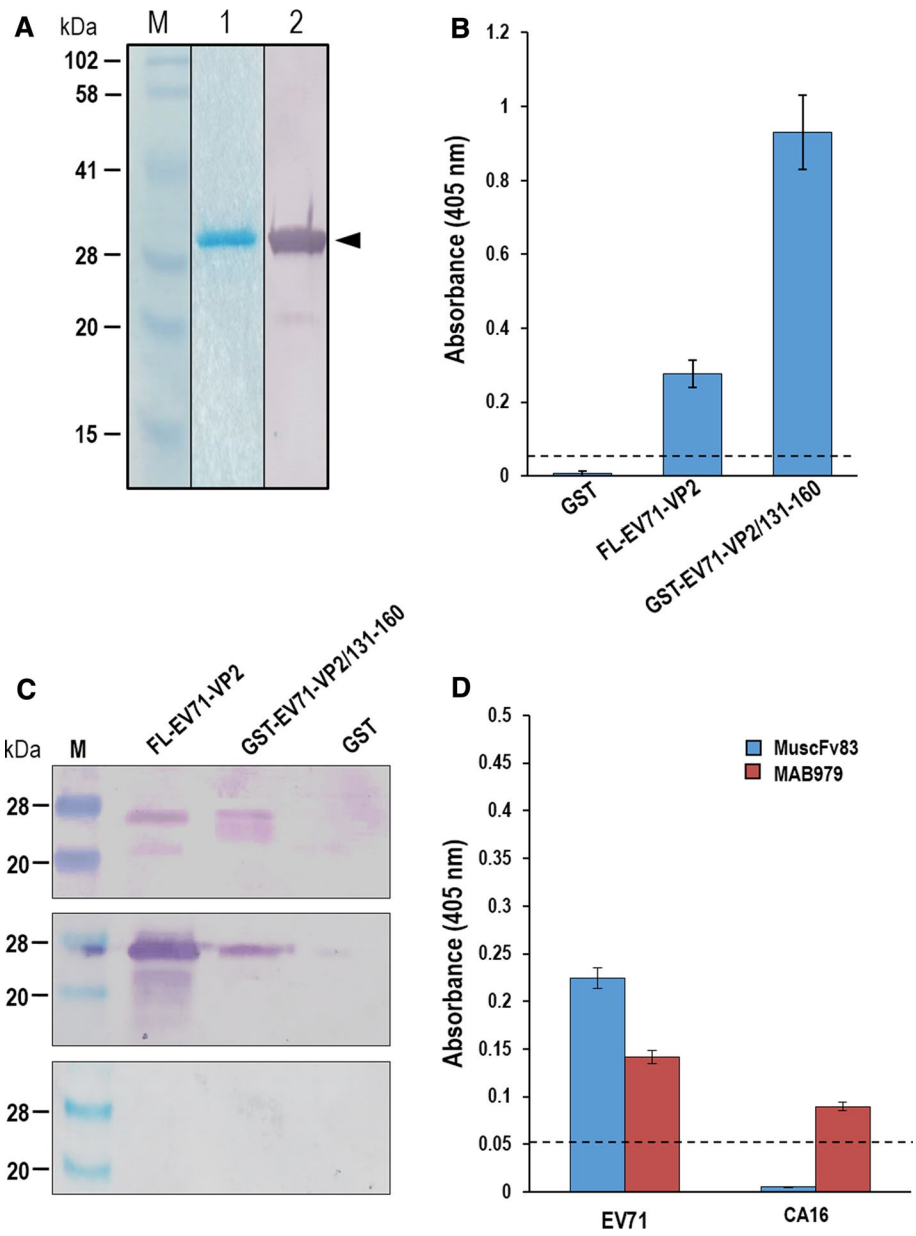

Fig. 3 Antigenic specificity of MuscFv83. **A** SDS-PAGE-separated MuscFv83 (lane 1) and SDS-PAGE-separated MuscFv83 probed with anti-c-Myc (lane 2). **B** MuscFv83 bound to FL-EV71-VP2 and GST-EV71-VP2/131-160 (by indirect ELISA). **C** MuscFv83 bound to FL-EV-71-VP2 and GST-EV71-VP2/131-160, but did not bind to GST (by Western blotting; upper panel). The positive controls were MAB979 bound to FL-EV71-VP2 and GST-EV71-VP2/131-160 (middle panel). Antigens probed with diluent were used as negative controls (lower panel) (M, molecular weight marker). **D** MuscFv83 bound to EV71 particles, but did not bind to CA16 particles. MAB979 caused cross-reactivity with CA16

to the beads by the GST molecule should allow the EV71-VP2 peptide portion to become more prominent and easily accessible by specific phages in the library. Given that MuscFv83 produced the highest binding signal to EV71-VP2 and GST-EV71-VP2/131-160, the coding sequence of this antibody was subcloned from phagemid to plasmid for larger scale production of soluble antibodies. Soluble MuscFv83 produced by plasmid-transformed *E. coli* retained its binding activity to GST-EV71-VP2/131-160 and FL-EV71-VP2, and to EV71 particles, but did not bind to GST or CA16. This indicates that MuscFv83 is specific for EV71-VP2. EV71-VP2/131-160 is located on the VP2-EF loop (amino acid residues 136-150), which is surface exposed [36]; thus, it should be easily accessible by MuscFv83. Computerized docking models revealed that MuscFv83 used both VH and VL cooperatively in target binding (using different interactive bonds) to multiple, specific residues of EV71-VP2, while MuscFv63 and MuscFv82 used only the VH domain to interact with fewer residues in the EV71-VP2/131-160 peptide. The 3D structures of EV71-VP2 and CA16-VP2 were overlaid to define the VP2 antigenic peptide that prevents cross-reactivity between MuscFv83 and CA16-VP2. Figure 1D shows that even though the overall 3D structure of VP2 of both EV71 and CA16 is compact and similar,

Table 2 Residues of EV71-VP2 peptide bound by the residues and domains of MuscFvs

EV71-VP2 residue	MuscFv63		Interactive bond
Amino acid	Amino acid	Domain	
H145	T104	VH-CDR3	NH-π
P146	R103	VH-CDR3	Van de Waals
Y148	Y109	VH-CDR3	π–π interaction
K149[a]	N31	VH-CDR1	Salt-bridge
T151	R103	VH-CDR3	H-bond
Q152	Y57	VH-CDR2	H-bond
P153	Y57	VH-CDR2	Hydrophobic
D156[a]	K58	VH-CDR2	Salt-bridge
G157	N55	VH-CDR2	H-bond
E159[a]	Y54	VH-CDR2	H-bond
L160	Y54	VH-CDR2	Hydrophobic
	MuscFv82		Interactive bond
	Amino acid	Domain	
G133	Y57	VH-CDR2	Hydrophobic
T134	Y57	VH-CDR2	OH-π
V135[a]	Y60	VH-CDR2	OH-π
	K58	VH-CDR2	Hydrophobic
E142	K58	VH-CDR2	H-bond
S144	K58	VH-CDR2	H-bond
H145	N55	VH-CDR2	H-bond
P147	N55	VH-CDR2	Hydrophobic
Y148	Y54	VH-CDR2	π–π interaction
K149[a]	N31	VH-CDR2	H-bond
Q150[a]	Y57	VH-CDR2	Hydrophobic
P153	K102	VH-CDR3	Hydrophobic
D156[a]	K102	VH-CDR3	H-bond
	MuscFv83		Interactive bond
	Amino acid	Domain	
T134	Y101	VH-CDR3	Van de Waals
V135[a]	T30	VH-CDR1	CH-π
E142	Y32	VH-CDR1	OH-π
S144	Y101	VH-CDR3	Van de Waals
H145	Y101	VH-CDR3	H-bond
K149[a]	Y186	VL-FR2	H-bond
Q150[a]	G102	VH-CDR3	Hydrophobic
	Y101	VH-CDR3	OH-π
P153	R103	VH-CDR3	CH-π
D156[a]	N169	VL-CDR1	H-bond
G157	R103	VH-CDR3	H-bond
F158[a]	R103	VH-CDR3	NH-π
E159[a]	Y233	VL-CDR3	Van de Waals

[a]Amino acids in bold are conserved for EV71-VP2

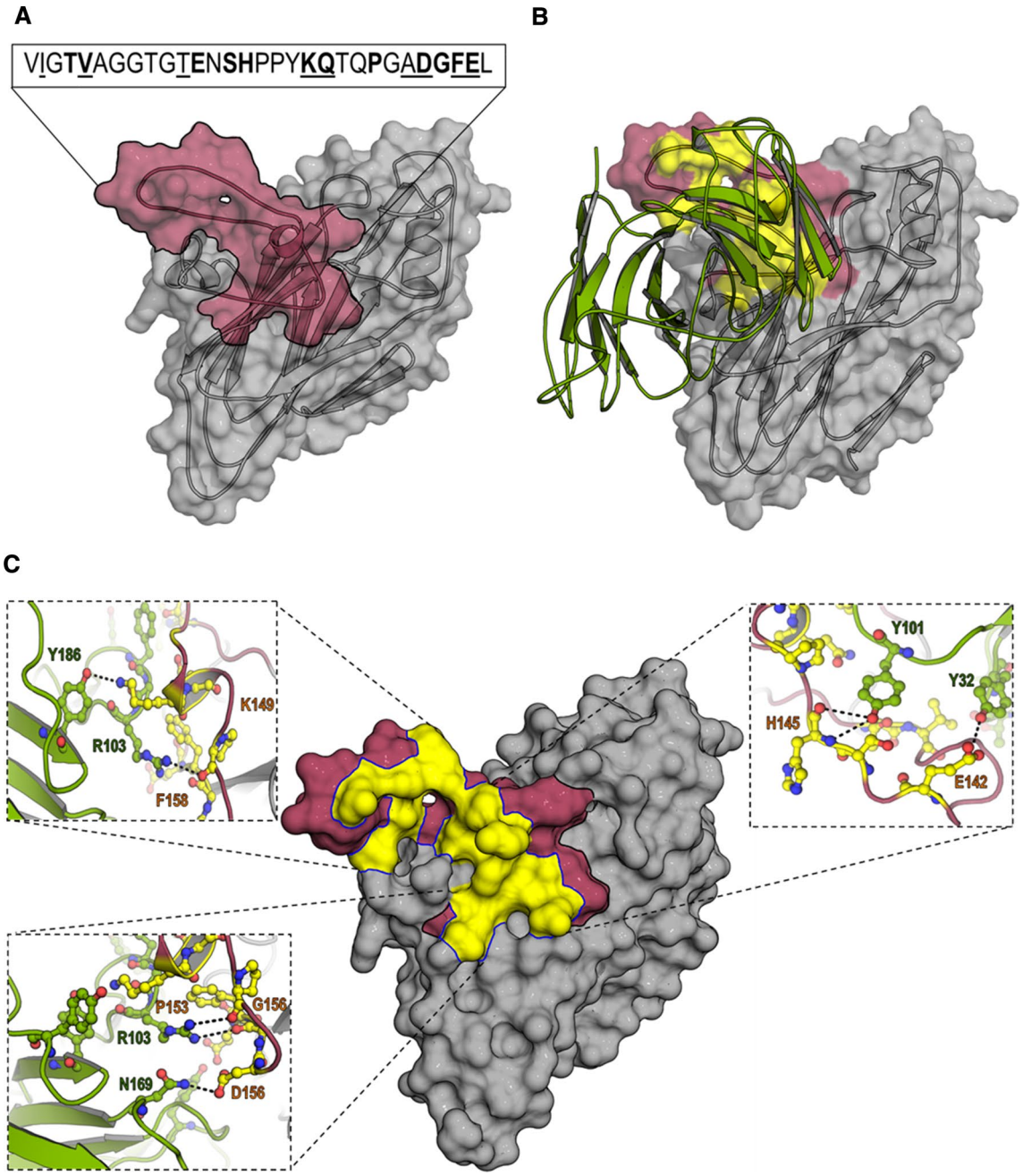

Fig. 4 Computerized interactions between modeled-EV71-VP2 (genotype B5) and MuscFv83 with focus on interactive residues. **A** EV71-VP2 (grey) showing the region predicted to contain the B-cell epitope (red). The sequence of the EV71-VP2 peptide is boxed, the EV71-VP2-specific residues are underlined, and the residues that were predicted to form contact interfaces with MuscFv83 are in bold. **B** CDR loops protrude from MuscFv83 (green) to interact with the EV71-VP2 B-cell epitope (yellow). **C** Interactive residues between MuscFv83 (green) and specific residues of EV71-VP2. H-bonds are indicated by grey-colored dots

the spatial arrangement of critical residues in the predicted linear epitope differs. We suspect this is the reason why MuscFv83 does not bind to VP2 from CA16. The results of this study suggest that MuscFv83 has high potential as a specific diagnostic/detection reagent for EV71 during point-of-care case diagnosis and outbreak recognition.

Acknowledgements Funding was provided by grants from the following sources: Thailand Research Fund (MRG5680105); Thammasat University (Project IDs 218028, 180630, and 151632); Center of Excellence in Clinical Virology (GCE 58-014-30-004); Research Chair Grant (P-15-50004); and, NSTDA Chair Professor Grant (P-1450624). The authors gratefully acknowledge Ms Jiratchaya Puenpa of Chulalongkorn University for EV71 propagation.

Compliance with ethical standards

Consent for publication All authors consent to publication.

Conflict of interest All authors declare no personal or professional conflicts of interest, and no financial support from the companies that produce and/or distribute the drugs, devices, or materials described in this report.

Animal ethics Institutional guidelines for the care and use of animals were followed.

Ethics approval and informed consent This article does not contain any studies with human participants performed by any of the authors.

References

1. AbuBakar S, Chee HY, Al-Kobaisi MF, Xiaoshan J, Chua KB, Lam SK (1999) Identification of enterovirus 71 isolates from an outbreak of hand, foot and mouth disease (HFMD) with fatal cases of encephalomyelitis in Malaysia. Virus Res 61:1–9
2. Breitling F, Broders O, Helmsing S, Hust M, Dübel S (2010) Human antibody gene libraries. In: Kontermann R, Dübel S (eds) Antibody Engineering, vol 1, 2nd edn. Springer, Heidelberg, pp 197–206
3. Brochet X, Lefranc MP, Giudicelli V (2008) IMGT/V-QUEST: the highly customized and integrated system for IG and TR standardized V-J and V-D-J sequence analysis. Nucleic Acids Res 36:W503–W508 **(Web Server issue)**
4. Casas I, Palacios GF, Trallero G, Cisterna D, Freire MC, Tenorio A (2001) Molecular characterization of human enteroviruses in clinical samples: comparison between VP2, VP1, and RNA polymerase regions using RT nested PCR assays and direct sequencing of products. J Med Virol 65:138–148
5. Chen TC, Chen GW, Hsiung CA, Yang JY, Shih SR, Lai YK, Juang JL (2006) Combining multiplex reverse transcription-PCR and a diagnostic microarray to detect and differentiate enterovirus 71 and coxsackievirus 16. J Clin Microbiol 44:2212–2219
6. Chiang PS, Huang ML, Luo ST, Lin TY, Tsao KC, Lee MS (2012) Comparing molecular methods for early detection and serotyping of enteroviruses in throat swabs of pediatric patients. PLoS One 7:e48269
7. FG-MD: high-resolution proteins structure refinement by fragment-guided MD simulation. Available online: http://zhanglab.ccmb.med.umich.edu/FG-MD/ Accessed 1 June 2017
8. Huang ML, Chiang PS, Luo ST, Liou GY, Lee MS (2010) Development of a high-throughput assay for measuring serum neutralizing antibody against enterovirus 71. J Virol Methods 165:42–45
9. Hust M, Dübel D (2010) Human antibody gene libraries. In: Kontermann R, Dübel S (eds) Antibody Engineering, vol 1, 2nd edn. Springer, Heidelberg, pp 65–84
10. I-TASSER Online. Protein Structure & Function Prediction—Google Search. Available online: http://zhanglab.ccmb.med.umich.edu/I-TASSER/ Accessed 1 June 2017
11. Keawcharoen J (2012) Hand, foot, and mouth disease. Thai J Vet Med 42:255–257
12. Kiener TK, Jia Q, Lim XF, He F, Meng T, Chow VT, Kwang J (2012) Characterization and specificity of the linear epitope of the enterovirus 71 VP2 protein. Virol J 9:55
13. Koh WM, Bogich T, Siegel K, Jin J, Chong EY, Tan CY, Chen MI, Horby P, Cook AR (2011) The epidemiology of hand, foot and mouth disease in Asia: A systematic review and analysis. Pediatr Infect Dis J 35:e285–e300
14. Kozakov D, Beglov D, Bohnuud T, Mottarella SE, Xia B, Hall DR, Vajda S (2013) How good is automated protein docking? Protein 81:2159–2166
15. Kulkeaw K, Sakolvaree Y, Srimanote P, Tongtawe P, Maneewatch S, Sookrung N, Tungtrongchitr A, Tapchaisri P, Kurazono H, Chaicumpa W (2009) Human monoclonal ScFv neutralize lethal Thai cobra, *Naja kaouthia*, neurotoxin. J Proteomics 72:270–282
16. Larsen JE, Lund O, Nielsen M (2006) Improved method for predicting linear B-cell epitopes. Immunome Res 2:2
17. Laskowski RA, MacArthur MW, Moss DS, Thornton JM (1993) PROCHECK: a program to check the stereochemical quality of protein structures. J Appl Cryst 26:283–291
18. Lin Y, Wen K, Pan Y, Wang Y, Che X, Wang B (2011) Cross-reactivity of anti-EV71 IgM and neutralizing antibody in series sera of patients infected with enterovirus 71 and coxsackievirus A 16. J Immunoassay Immunochem 32:233–243
19. Liu CC, Chou AH, Lien SP, Lin HY, Liu SJ, Chang JY, Guo MS, Chow YH, Yang WS, Chang KH, Sia C, Chong P (2011) Identification and characterization of a cross-neutralization epitope of enterovirus 71. Vaccine 29:4362–4372
20. Miao LY, Pierce C, Gray-Johnson J, DeLotell J, Shaw C, Chapman N, Yeh E, Schnurr D, Huang YT (2009) Monoclonal antibodies to VP1 recognize a broad range of enteroviruse. J Clin Microbiol 47:3108–3113
21. ModRefiner: High-resolution protein structure refinement and relaxation by energy minimization. Available online: http://zhanglab.ccmb.med.umich.edu/ModRefiner/ Accessed 1 June 2017
22. Moon SA, Ki MK, Lee S, Hong ML, Kim M, Kim S, Chung J, Rhee SG, Shim H (2011) Antibodies against non-immunizing antigens derived from a large immune scFv library. Mol Cells 31:509–513
23. Nix WA, Oberste MS, Pallansch MA (2006) Sensitive, seminested PCR amplification of VP1 sequences for direct identification of all enterovirus serotypes from original clinical specimens. J Clin Microbiol 44:2698–2704
24. Oberste MS, Maher K, Kilpatrick DR, Flemister MR, Brown BA, Pallansch MA (1999) Typing of human enteroviruses by partial sequencing of VP1. J Clin Microbiol 37:1288–1293
25. Puenpa J, Theamboonlers A, Korkong S, Linsuwanon P, Thongmee C, Chatproedprai S, Poovorawan Y (2011) Molecular characterization and complete genome analysis of human enterovirus 71 and coxsackievirus A16 from children with hand, foot and mouth disease in Thailand during 2008–2011. Arch Virol 15:2007–2013
26. Reed Z, Cardosa MJ (2016) Status of research and development of vaccines for enterovirus 71. Vaccine 34:2967–2970
27. Romero JR (1999) Reverse-transcription polymerase chain reaction detection of the enteroviruses. Arch Pathol Lab Med 123:1161–1169
28. Singh S, Chow VT, Phoon MC, Chan KP, Poh CL (2002) Direct detection of enterovirus 71 (EV71) in clinical specimens from a hand, foot, and mouth disease outbreak in Singapore by reverse transcription-PCR with universal enterovirus and EV71-specific primers. J Clin Microbiol 40:2823–2827
29. Smith GP (1985) Filamentous fusion phage: novel expression vectors that display cloned antigens on the virion surface. Science 228:1315–1317

30. Solomon T, Lewthwaite P, Perera D, Cardosa MJ, McMinn P, Ooi MH (2010) Virology, epidemiology, pathogenesis, and control of enterovirus 71. Lancet Infect Dis 10:778–790
31. Strebe N, Breitling F, Moosmayer D, Brocks B, Dübel S (2010) Cloning of variable domains from mouse hybridoma by PCR. In: Kontermann R, Dübel S (eds) Antibody Engineering, vol 1, 2nd edn. Springer, Heidelberg, pp 3–14
32. Thanongsaksrikul J, Srimanote P, Maneewatch S, Choowongkomon K, Tapchaisri P, Makino S, Kurazono H, Chaicumpa W (2010) A V_HH that neutralizes the zinc metalloproteinase activity of botulinum neurotoxin type A. J Biol Chem 285:9657–9666
33. Thoelen I, Lemey P, Van Der Donck I, Beuselinck K, Lindberg AM, Van Ranst M (2003) Molecular typing and epidemiology of enteroviruses identified from an outbreak of aseptic meningitis in Belgium during the summer of 2000. J Med Virol 70:420–429
34. Tsao LY, Lin CY, Yu YY, Wang BT (2006) Microchip, reverse transcription-polymerase chain reaction and culture methods to detect enterovirus infection in pediatric patients. Pediatr Int 48:5–10
35. Van Doornum GJ, De Jong JC (1998) Rapid shell vial culture technique for detection of enteroviruses and adenoviruses in fecal specimens: comparison with conventional virus isolation method. J Clin Microbiol 36:2865–2868
36. Wang X, Peng W, Ren J, Hu Z, Xu J, Lou Z, Li X, Yin W, Shen X, Porta C, Walter TS, Evans G, Axford D, Owen R, Rowlands DJ, Wang J, Stuart DI, Fry EE, Rao Z (2012) A sensor-adaptor mechanism for enterovirus uncoating from structures of EV71. Nat Struct Mol Biol 19:424–429
37. World Health Organization (2004) Polio Laboratory Manual 4th ed. Immunization, Vaccines and Biological. http://apps.who.int/iris/bitstream/10665/68762/1/WHO_IVB_04.10.pdf. Accessed 8 August 2017
38. World Health Organization (2011) A guide to clinical management and public health response for hand, foot and mouth disease (HFMD). http://www.wpro.who.int/publications/docs/GuidancefortheclinicalmanagementofHFMD.pdf. Accessed 8 August 2017
39. Yip CCY, Lau SK, Woo PC, Yuen KY (2013) Human enterovirus 71 epidemics: what's next? Emerg Health Threats J 6:19780
40. Yuan Q, Huang L, Wang X, Wu Y, Gao Y, Li C, Nian S (2012) Construction of human nonimmune library and selection of scFvs against IL-33. Appl Biochem Biotechnol 167:498–509